융기 도파관 내의 전계 분포와 커플링에 대한 분석

권 광희, 이 승학, 이 경보, 이 원창, 구 본엽, 손 현
경북대학교 전자전기공학부
대구광역시 북구 산격동 1370 번지
trec@palgong.kyungpook.ac.kr

Analysis of Ridge Waveguide Field Description and Directional Couplers

K. H. Kwon, S. H. Lee, K. B. Lee, W. C. Lee, B. Y. Koo, H. Son
Kyungpook National University
School of Electronics and Electrical Engineering

Abstract

An application determination of the dominant-mode fields in ridge waveguides at all frequencies has been made. Evaluations of the fields along the walls of a commercially standard single-ridge guide having a usable frequency range from 3.75 to 15.0 Ge, This paper presented the analysis of the mode directive coupling characteristics of two ridge waveguide using mode matching techniques for TE_{10} mode.

I. INTRODUCTION

Ridged waveguides have been useful for several years in microwave systems requiring broadband operation. Hopfer used a quasi-static solution for the discontinuty susceptance between parallel plates obtained from Marcuvitz [1]. Little is said about the fields of ridged guide until 1961 when Getsinger [2] formulated approximate field equations by assuming a TEM mode at the gap and matching only the electric field. In designing ridge waveguide devices it is often helpful to know the relative values of the dominant mode fields components over the cross section of the ridge guide, especially those fields along the waveguide walls.

II. RELATION AMONG THE FIELD COMPONENTS

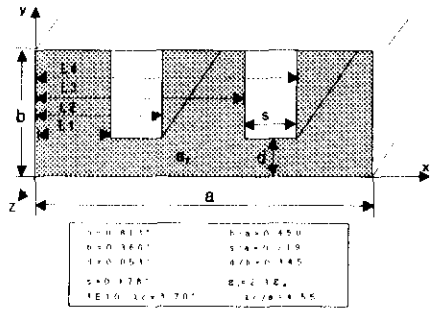

Fig. 1 Geometry of two ridge waveguide.

Consider a lossless cylinderical waveguide of arbitrary cross section, but whose electromagnetic boundary conditions are invariant under translation in

$$
\begin{aligned}
&\frac{1}{b}\int_0^b E_{y1}(l_1)dy = \frac{1}{b}\int_0^b E_{y2}(l_1)dy \\
&\left(\frac{2A_{n1}\gamma_{n1}}{\gamma_{n1}^2+k^2}\right)\left(n\pi/b\right)\sinh(\gamma_{n1}l_1) = \frac{1}{b}\int_0^b E_{y1}(l_1)\cos\left(n\pi y/b\right)dy \\
&\frac{1}{b}\int_0^b E_{y1}(x)dy = \frac{1}{b}\int_0^b E_{y3}(x_1)dy \text{ at } x=l_2 \text{ and } x=l_3 \\
&\frac{2}{b}\int_0^b E_{y1}(x)\cos\left(n\pi y/b\right)dy = \frac{2}{b}\int_0^b E_{y3}(x)\cos\left(n\pi y/b\right)dy \text{ at } x=l_2 \text{ and } x=l_3 \\
&\frac{2}{b}\int_0^b H_{y1}(x)\cos\left(n\pi y/b\right)dy = \frac{2}{b}\int_0^b H_{y3}(x)\cos\left(n\pi y/b\right)dy \text{ at } x=l_2 \text{ or } x=l_3 \\
&\frac{1}{b}\int_0^b E_{y2}(l_2)dy = \frac{1}{b}\int_0^b E_{y3}(l_2)dy \\
&A_{n2}\left(\frac{\gamma_{n2}}{\gamma_{n2}^2+k^2}\right)\left(\frac{n\pi}{b}\right)\left(e^{(\gamma_{n2}l_2+\alpha)}-e^{-(\gamma_{n2}l_2+\alpha)}\right)=\frac{2}{b}\int_0^b E_{y2}(l_2)\cos\left(n\pi y/b\right)dy
\end{aligned}
\qquad (6)
$$

When (4) has been substituted for E_y component in (5), and the integrations are carried out, it is found that

$$
\begin{aligned}
&A_{01} = E_0\frac{d\cos\left(k_c s/2\right)}{b\sin(k_c l_1)} \\
&A_{n1} = jE_0\frac{d}{b}\sin\left(k_c s/2\right)\left\{e^{-jk_c l_2}+\left(\frac{e^{-jk_c l_2}-e^{-jk_c l_3}}{e^{jk_c l_2}-e^{-jk_c l_3}}\right)e^{jk_c l_2}\right\}^{-1} \\
&B_{01} = -\left(\frac{e^{-jk_c l_2}-e^{jk_c l_3}}{e^{jk_c l_2}-e^{jk_c l_3}}\right)A_{01} \\
&A_{02} = E_0\frac{d\cos\left(k_c s/2\right)}{b_2\sin\left\{k_c(l_2-\alpha)\right\}} \\
&A_{n1} = E_0\frac{b_1\left(\gamma_{n1}^2+k_c^2\right)\cos\left(k_c s/2\right)\sin\left(n\pi d/b\right)}{(n\pi)^2\gamma_{n1}\sinh(\gamma_{n1}l_1)} \\
&A_{n2} = E_0\frac{2b}{(n\pi)^2}\sin\left(k_c s/2\right)\left\{e^{-\gamma_{n2}l_2}+\left(\frac{e^{\gamma_{n2}l_2}-e^{-\gamma_{n2}l_3}}{e^{\gamma_{n2}l_2}-e^{-\gamma_{n2}l_3}}\right)e^{\gamma_{n2}l_2}\right\}^{-1} \\
&B_{n2} = -\left(\frac{e^{\gamma_{n2}l_2}-e^{\gamma_{n2}l_3}}{e^{\gamma_{n2}l_2}-e^{\gamma_{n2}l_3}}\right)A_{n2} \\
&A_{n3} = E_0\left|\frac{2b_2\sin\left(k_c s/2\right)\sin\left(n\pi d/b\right)}{(n\pi)^2}\left(\frac{\gamma_{n3}^2+k_c^2}{k_c}\right)\right| \\
&\qquad\left\{e^{-\gamma_{n3}l_3}+\left(\frac{e^{-\gamma_{n3}l_2}-e^{\gamma_{n3}l_3}}{e^{\gamma_{n3}l_2}-e^{\gamma_{n3}l_3}}\right)e^{\gamma_{n3}l_3}\right\}^{-1}
\end{aligned}
\qquad (7)
$$

the fields at the cutoff frequency have been determined, and fields at other frequencies will now be found. Recognizing that

$$
k = 2\pi/\lambda,\quad k_c = 2\pi/\lambda_c,\quad k_z = \frac{2\pi}{\lambda}\sqrt{1-\left(\frac{\lambda}{\lambda_c}\right)^2} \qquad (8)
$$

where λ is free-space wavelength and λ_c is the cutoff wavelength, which can be found from Hofer's graphs, sufficient information is available to specify approximately all the electric and magnetic fields over the cross section of each ridge guide at any frequency. The approximate formulas, (5) and (7), for the fields in ridge waveguide were used to compute the relative field values along the inner surfaces of the two ridge described in Fig. 1. These fields have been plotted in Fig.4 for the single ridge and in Fig.5 for the two ridges. Notice that the following definitions have been used:

$$
e_x = \frac{E_x}{E_0},\quad e_y = \frac{E_y}{E_0}
$$
$$
h_x = -\eta\frac{kH_x}{k_c E_0},\quad h_y = -\eta\frac{kH_y}{k_c E_0},\quad h_z = -\eta\frac{k_z H_z}{k_c E_0} \qquad (9)
$$

IV. NUMERICAL RESULT AND CONCLUSION

The inside cross-sectional dimensions of both the ridge guides used are shown in Fig. 4,5, along with dimensional ratios and the cut-off wavelengths, as computed from Hopfer's curves.

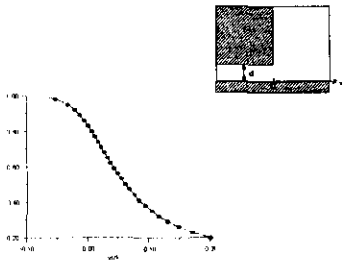

Fig. 3 Relative electric field along wall opposing corner.

The smooth curve for e_y, h_x in the ridge of the two ridge guide was achieved by replacing computed values for the vicinity of ridge with values taken from a static solution in Fig.3. For the electric field near

the axial direction. Relations among field components may be found by expanding Maxwell's curl equations for exponential variation in the z direction. For a TE wave, the following relations can be found:

$$\left.\begin{aligned} \frac{E_x}{H_y} &= -\frac{E_y}{H_x} = \eta\frac{k}{k_z} \\ H_z &= \frac{j}{k\eta}\left(\frac{\partial E_y}{\partial x} - \frac{\partial E_x}{\partial y}\right) \end{aligned}\right\} \quad (1)$$

At the cutoff frequency, the transverse-resonance condition can be imposed on the waveguide.

$$E_z = H_x = H_y = 0\ ,\ k_z = 0\ ,\ k^2 = k_c^2 \quad (2)$$

where k_c is the transverse, or cutoff, wave number in each regions. when expanded to the conditions of (2) and exponential propagation along x, yield the following relation between transverse electric fields

$$E_y = \left(\frac{\gamma_n}{\gamma_n^2 + k_c^2}\right)\frac{\partial E_x}{\partial y} \quad (3)$$

where γ_n is the propagation constant in the x-direction of any mode satisfying (2) in the chosen rectangular section at the cutoff frequency. For a specified TE mode, (1) and (2) can be used to determine all the electric and magnetic field components at any frequency if the y components of electric fields of the contributing transversely propagating modes are known over the cross section of the guide at the cutoff frequency.

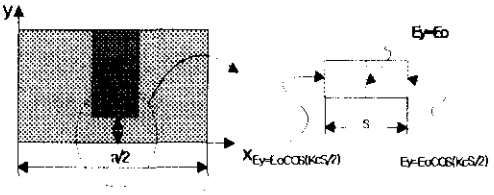

Fig.2 Equivalent structure analyzed.

III. DERIVATION OF THE WAVEGUIDE FIELDS

The electric field will be determined at the cut-off frequency. At the center of the ridge in Fig.2, the electric field is E_o and exists in the y direction only. Assuming only a TEM transmission-line mode in the gap under the ridge, the electric field at each edge of the ridge for this mode must be

$$\left.\begin{aligned} E_{yr} &= E_0\cos(k_c s/2), \quad 0 < y < d \\ E_{yr} &= 0, \qquad\qquad d < y < b \end{aligned}\right\} \quad (4)$$

For the cutoff TM waves $\left(H_x = H_y = 0\right)$, the assumed electric field along x of the TM mode has the form

$$\left.\begin{aligned} E_{y01} &= A_{01}\sin(k_c x) \\ E_{y03} &= A_{03}e^{-jk_c x} + B_{03}e^{jk_c x} \\ E_{y02} &= A_{02}\sin\{k_c(x-a)\} \end{aligned}\right\}$$

$$\left.\begin{aligned} E_{yn1} &= A_{n1}e^{-\gamma_{n1}x}\sin\left(n\pi y/b\right) + B_{n1}e^{\gamma_{n1}x}\sin\left(n\pi y/b\right) \\ E_{yn3} &= A_{n3}e^{-\gamma_{n3}x}\sin\left(n\pi y/b\right) + B_{n3}e^{\gamma_{n3}x}\sin\left(n\pi y/b\right) \\ E_{yn2} &= A_{n2}e^{-\gamma_{n2}x}\sin\left(n\pi y/b\right) + B_{n2}e^{\gamma_{n2}x}\sin\left(n\pi y/b\right) \end{aligned}\right\}$$

$$\left.\begin{aligned} E_{yn1} &= \left(\frac{\gamma_{n1}}{\gamma_{n1}^2 + k_c^2}\right)\frac{n\pi}{b}\cos\left(n\pi y/b\right)\left(B_{n1}e^{\gamma_{n1}x} - A_{n1}e^{-\gamma_{n1}x}\right) \\ E_{yn3} &= \left(\frac{\gamma_{n3}}{\gamma_{n3}^2 + k_c^2}\right)\frac{n\pi}{b}\cos\left(n\pi y/b\right)\left(B_{n3}e^{\gamma_{n3}x} - A_{n3}e^{-\gamma_{n3}x}\right) \\ E_{yn2} &= \left(\frac{\gamma_{n2}}{\gamma_{n2}^2 + k_c^2}\right)\frac{n\pi}{b}\cos\left(n\pi y/b\right)\left(B_{n2}e^{\gamma_{n2}x} - A_{n2}e^{-\gamma_{n2}x}\right) \end{aligned}\right\} \quad (5)$$

where γ_{n1}, γ_{n3} and γ_{n2} are each propagation constant in the x direction for the n-th mode, And A_{n1}, A_{n2}, A_{n3}, B_{n1}, B_{n2} and B_{n3} are constants in each regions. by matching its electric field at the edge of the each ridge to the electric field of a TEM transmission-line mode plus higher order, cutoff TM modes propagating transversely in each large end sections, we can obtain constants in each regions.

very closely ridge-angle bend near a ground plane, The static solution was used only over a small distance, compared to any wavelength in the guide operating range.

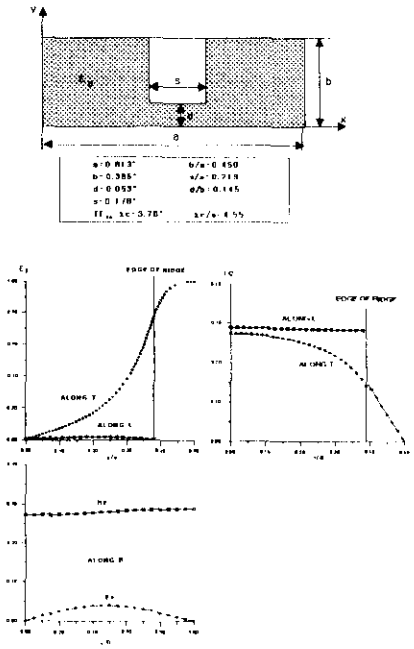

Fig. 4 Peripheral fields with the single ridge.

In as much as a static field has no curl, Its use required a little change in the computed values of the longitudinal magnetic field The graph of magnetic field shows only a small step between the solution under the ridge and the solution of the end-section, and so it is believed that the curve for magnetic field is a reasonably good approximation to the actual longitudinal magnetic field near the ridge, as well as away from it.

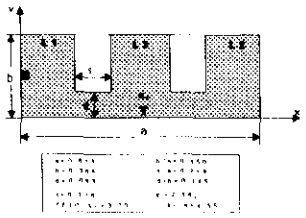

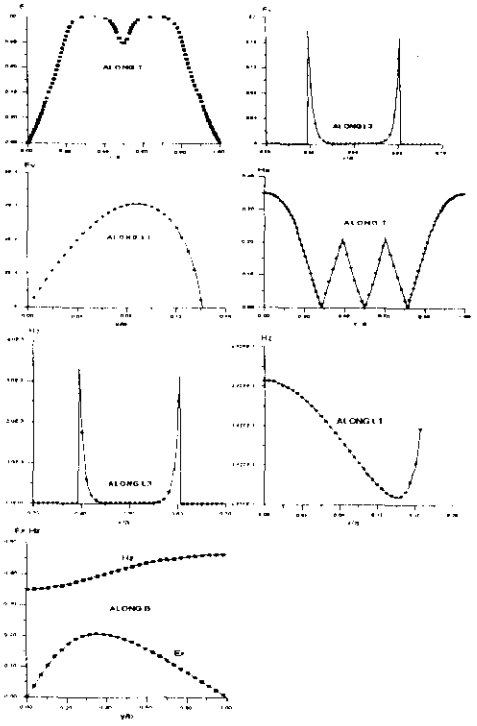

Fig. 5 Peripheral fields with two ridge.

V. REFERENCES

[1] N. Marcuvitz, Waveguide handbook. M. I. T. Rad. Lab. Ser., vol. 10. New York: McGraw-Hill, 1951, pp. 399-402.

[2] W. J. Getsinger, "ridged waveguide field description and application to directional couplers," IRE Trans. Microwave Theory Tech., vol. MTT-10, Jan. 1962, pp. 41-50.

[3] S. B. Cohn, "Properties of ridged wave guide," Proc. IRE, vol. 35, Aug. 1947, pp. 783-788.

[4] S. Hoper, "The design of ridged wave guides," IRE Trans. Microwave Theory Tech., vol. MTT-3, Oct. 1955, pp. 20-29.

[5] J. R. Pyle, "The cutoff wavelength of the TE_{10} mode in ridged Microwave Theory Tech., vol. MTT-14, Apr. 1966, pp. 175-183.